Thermodynamics and Kinetics of Formation of the Alkaline State of a Lys 79→Ala/Lys 73→His Variant of Iso-1-cytochrome *c*†

Saritha Baddam and Bruce E. Bowler*

Department of Chemistry and Biochemistry, University of Denver, 2190 East Iliff Avenue, Denver, Colorado 80208-2436

Received August 10, 2005

ABSTRACT: The alkaline transition kinetics of a Lys 73→His (H73) variant of iso-1-cytochrome *c* are triggered by three ionizable groups [Martinez, R. E., and Bowler, B. E. (2004) *J. Am. Chem. Soc. 126*, 6751−6758]. To eliminate ambiguities caused by overlapping phases due to formation of the Lys 79 alkaline conformer and proline isomerization associated with the His 73 alkaline conformer, we mutated Lys 79 to Ala in the H73 variant (A79H73). The stability and guanidineHCl *m*-values of the A79H73 and H73 variants at pH 7.5 are the same. The Ala 79 mutation causes formation of the alkaline conformer to depend on [NaCl]. The salt dependence saturates at 500 mM NaCl, and the thermodynamics of alkaline state formation for the A79H73 and H73 variants become identical. The salt dependence is consistent with loss of an electrostatic contact between Lys 79 and heme propionate D in the A79H73 variant. The kinetics of alkaline state formation for the A79H73 variant support the three trigger group model developed for the H73 variant, with the primary trigger, pK_{HL}, being ionization of His 73. The low pH ionization, pK_{H1}, is perturbed by the Ala 79 mutation indicating that this ionization is modulated by the buried hydrogen bond network involving heme propionate D. The A79H73 variant has a high spin heme above pH 9 suggesting that the high pH ionization, pK_{H2}, involves a high spin heme conformer. The proline isomerization phase is modulated by both pK_{HL} and pK_{H2} indicating that it is sensitive to protein conformation.

In 1941, Theorell and Åkesson (*1*) showed that horse ferricytochrome *c* has five pH dependent conformational states linked by protonation events corresponding to four distinct p*K* values as follows:

Ferricytochrome *c*	State:	I →	II →	III →	IV →	V
	pK:		0.4	2.5	9.35	12.8

The native state is state III. The acid transition (state III → II) in ferricytochrome *c* is complex, involving two or three protons (*2*). The transition from state III to IV called the alkaline transition was noted by Theorell and Åkesson (*1*) to be associated with the reduction of an absorption band at 695 nm having a low extinction coefficient. This band and the associated phenomenon of the alkaline transition have been universally found in both prokaryote and eukaryote ferricytochromes *c* (*3*). The alkaline transition involves one proton. In the wild type (WT)[1] yeast iso-1-cytochrome *c*, the ligands replacing Met 80 during the alkaline transition are known to be lysines 73 and 79 (*4*, *5*).

A number of recent studies (*6*−*10*) have demonstrated a linkage between the properties of the alkaline conformer of cytochrome *c* and the unfolding of a substructure of cytochrome *c* that encompasses residues 70 to 85 of the protein (*11*, *12*). This portion of the protein forms a surface loop which sits above the Met 80 ligand of the heme. Since this surface loop is believed to gain structure late in the folding of this protein (*11*), the alkaline conformer is of interest as a stable model for a late folding intermediate. Another important aspect of the alkaline conformer of cytochrome *c* is that the heme ligand exchange reaction which results (Met 80→Lys in the WT protein or Met 80→His for variants studied in this lab) causes a dramatic drop in the reduction potential of the heme (*5*). Thus, this conformer can act as an electron transfer gate (*13*−*18*), and may serve to modulate the flow of electrons through the electron transport chain (*5*, *19*, *20*).

In previous studies, we have demonstrated that a Lys 73→His (H73) variant of iso-1-cytochrome *c* leads to a partial unfolding of iso-1-cytochrome *c* near physiological pH that is analogous to the alkaline transition of the protein (*6*−*9*). Partial unfolding experiments done on this variant show a biphasic alkaline transition. Met 80 in the sixth coordination site of the heme begins to be replaced by His 73 near pH 6.0. The His 73−heme "alkaline" conformer reaches a maximal population of ∼30% near pH 7.5. Above this pH, Lys 79 binds to the heme replacing both His 73 and Met 80 as ligands. H73 iso-1-cytochrome *c* has allowed the extent of exposure of buried surface area in the alkaline conformer to be characterized (*6*, *8*, *9*), and recent kinetic studies have provided new insight into the triggering mechanism of the alkaline conformational transition (*21*) and the

† This work was supported by NSF Grant CHE 0316378 (B.E.B.). The Applied Photophysics π*-180 spectrometer was purchased with NIH Grant 1 S10 RR16632-01.

* To whom correspondence should be addressed. Phone: (303) 871-2985. Fax: (303) 871-2254. E-mail: bbowler@du.edu.

[1] Abbreviations: WT, wild-type iso-1-cytochrome *c* containing the mutation Cys 102→Ser; A79H73, variant of iso-1-cytochrome *c* carrying Lys 73→His and Lys 79→Ala mutations; H73, variant of iso-1-cytochrome *c* carrying a Lys 73→His mutation; CD, circular dichroism spectroscopy; gdnHCl, guanidine hydrochloride.

10.1021/bi0515873 CCC: $30.25
Published on Web 10/22/2005

role of this conformer in electron transfer gating (*18*).

While the H73 variant has been useful, the presence of Lys 79 complicates analysis of the partial unfolding caused by His 73−heme ligation during the alkaline conformational transition of this protein. In particular, the kinetic phases due to the Lys 79−heme conformer and a proline isomerization linked to the His 73−heme conformer occur on a similar time scale at some pHs, making the assignment of and analysis of the pH dependence of these kinetic phases somewhat ambiguous. To simplify the partial unfolding of the H73 variant, Lys 79 was replaced by Ala in the H73 variant, producing an A79H73 variant, which eliminates the Lys 79−heme alkaline conformer. Interestingly, we find that removal of Lys 79 leads to salt dependent effects on the partial unfolding of this protein which are consistent with the Lys 79 residue providing electrostatic stabilization of the native state relative to the alkaline state of the protein. We have also studied the acid transition of the A79H73 variant. As noted above, acid unfolding of cytochrome *c* is typically a 2 to 3 proton process. In the acid unfolding of the A79H73 variant, uptake of only ∼1 proton is observed at 695 nm, again indicating that the Lys 79→Ala substitution has an important impact on the electrostatics of iso-1-cytochrome *c*.

MATERIALS AND METHODS

Preparation of the A79H73 Variant. The A79H73 variant was produced by the unique restriction site elimination site-directed mutagenesis method (*22*) using the pRS/C7.8 phagemid vector carrying the H73 variant, as previously described (*23*). The H73 variant also contains the Cys 102→Ser mutation to prevent intermolecular disulfide dimerization during physical studies. The K79A primer (5′-d(CAAAGGCCATAGCGGTACCAGG)-3′, the mutation site in the oligonucleotide is underlined) was purchased from Biosynthesis, Inc. (Lewisville, TX). The selection primer was SacI-II+ (*23*), which eliminates a unique *Sac*I restriction enzyme site (and restores a *Sac*II site) upstream from the iso-1-cytochrome *c* gene, *CYC1*, in the pRS/C7.8 phagemid. pRS/C7.8 DNA isolated (Promega, Wizard SV+ miniprep kit) from *Escherichia coli*, containing DNA from the mutagenesis reaction, was first screened by carrying out *Sac*I and *Sac*II restriction enzyme digests and then sequenced by PCR methods (Quick Start kit, Beckman Coulter, Inc.). The sequencing reactions were then analyzed with a Beckman-Coulter CEQ XLS 8000 capillary electrophoresis autosequencer.

Phagemid DNA was transformed into the GM-3C-2 strain (*24*) of the yeast *Saccharomyces cerevisiae*, which lacks cytochrome *c*, by the LiCl method (*25*). Using previously described methods (*26*), the transformed yeast were characterized by phenotypic screening, a curing procedure to ensure phagemid-based expression, and phagemid recapture followed by DNA sequencing to be certain that no additional mutations were introduced into the *CYC1* gene under the conditions of selective pressure used to express iso-1-cytochrome *c* in *S. cerevisiae*. Protein was isolated and purified from *S. cerevisiae* as previously described (*27*−*29*).

Oxidation of Protein. Cytochrome *c* was oxidized by adding 5 mg of $K_3Fe(CN)_6$ per mg of protein and incubating at 4 °C for 1 h. It was then run through a G-25 size exclusion column which was preequilibrated with buffer appropriate to the experiment to remove the oxidizing agent. After collecting the protein, its concentration and degree of oxidation were determined, as previously described (*29*).

Guanidine Hydrochloride Denaturation Monitored by Circular Dichroism Spectroscopy. Global stability of the protein was determined by guanidine hydrochloride (gdnHCl)[1] denaturation monitored by circular dichroism (CD) spectroscopy using the Applied Photophysics π*-180 spectrometer. The experiments were done in 20 mM Tris, 40 mM NaCl (CD buffer) at pH 7.5 with 4 μM protein concentration at 25 °C. A 6 M gdnHCl stock solution was prepared containing the same CD buffer, and its concentration was determined using refractive index measurements (*30*). The ellipticity was measured at 222 nm, and 250 nm was used as a baseline. The experiments were performed using a two syringe Hamilton MicroLab 500 titration unit, as described previously (*27*, *31*). The ellipticity observed at 222 nm as a function of gdnHCl concentration was fit to eq 1 (*26*), which assumes a linear free energy relationship and

$$\theta = \frac{\theta^{o}_{N} + [(\theta^{o}_{D} + m_{D}[\text{gdnHCl}])\exp\{(m[\text{gdnHCl}] - \Delta G^{o}_{u}(H_2O))/RT\}]}{1 + \exp\{(m[\text{gdnHCl}] - \Delta G^{o}_{u}(H_2O))/RT\}} \quad (1)$$

two-state unfolding (*30*, *32*), where θ is the ellipticity of the sample, θ^{o}_{N} is the ellipticity of native protein, θ^{o}_{D} is the ellipticity of denatured protein at 0 M gdnHCl, m_D is the denaturant dependence of the denatured state ellipticity, m is the gdnHCl concentration dependence of the free energy of unfolding, ΔG_u, and $\Delta G^{o}_{u}(H_2O)$ is the free energy of unfolding extrapolated to 0 M gdnHCl. A set of three titrations were done, and the parameters were averaged.

Partial Unfolding by GdnHCl Monitored at 695 nm. Partial unfolding of the protein using gdnHCl was monitored at 695 nm, the band sensitive to the presence of the heme−Met 80 ligation (*3*). The experiments were carried out, as previously described (*31*), using about 200 μM protein at pH 7.5 and a Beckman DU 640 spectrophotometer. Absorbance at 750 nm was used as the background wavelength. The experiments were done in 20 mM Tris, pH 7.5, with various concentrations of NaCl (40, 100, 200, and 500 mM) at 25 °C. The data at various salt concentrations were fit to eq 2, where

$$A_{695} = \frac{A_N + [A_D{*}\exp\{(m[\text{gdnHCl}] - \Delta G^{o}_{u}(H_2O))/RT\}]}{1 + \exp\{(m[\text{gdnHCl}] - \Delta G^{o}_{u}(H_2O))/RT\}} \quad (2)$$

A_N and A_D are the absorbance values at 695 nm of the Met 80 bound native state and the denatured state, respectively. The equation assumes that the dependence of ΔG_u on [gdnHCl] is linear and that the protein unfolding can be approximated as a two state process (*30*, *32*). After fitting data at different salt concentrations to eq 2, a baseline correction was done to account for differences in protein concentration and background absorbance. The value for parameter A_D obtained as a result of fitting the data to eq 2 for 200 mM NaCl data was taken as a reference point, and A_D values at all other salt concentrations were adjusted to the same value assuming that the absorbance value of the

denatured state at any salt concentration is the same. For this purpose, A_D was first calculated at all other salt concentrations as $A_{D,S} = A_{D,200}([Cytc]_S/[Cytc]_{200})$ where $A_{D,S}$ is the calculated absorbance in the denatured state for other salt concentrations (other than 200 mM NaCl), $A_{D,200}$ is the absorbance value of denatured state at 200 mM salt concentration obtained from eq 2, $[Cytc]_S$ is the concentration of protein solution at a particular NaCl concentration, and $[Cytc]_{200}$ is the concentration of protein solution at 200 mM NaCl. Then, to correct for differences in background absorbance, the difference between the calculated ($A_{D,S}$) and observed A_D values (by fitting data to eq 2) was taken and that value was either subtracted from or added to the whole data set at each salt concentration, depending on whether the calculated $A_{D,S}$ value is lesser or greater than the actual observed A_D value. The absorbance values obtained as a result of this correction were then converted into molar extinction coefficient values and fit to eq 2 where the extinction coefficients of the native, ϵ_N, and denatured state, ϵ_D, replace A_N and A_D, respectively, in eq 2.

pH Titration Experiments. The alkaline transition of the protein was monitored by measuring the absorbance at 695 nm as a function of pH. The experiments were done in both 100 and 500 mM NaCl at 22 ± 1 °C at about 200 μM protein concentration. The sample was prepared by diluting 1 mL of the 2x protein (~400 μM protein in either 200 mM or 1 M NaCl) with 1 mL of ddH_2O. The solution was mixed with a 1000 μL pipet and the pH adjusted to about 2 by adding equal amounts of 2x protein and 3 M HCl solution. The pH was measured with an Accumet AB15 pH meter (Fisher Scientific) using an Accumet semimicro calomel pH probe (Fisher Scientific, Cat. No. 13-620-293). A volume of 70 μL of the protein sample was transferred to a microcell and the absorbance measured from 500 to 750 nm. Then, the solution from the microcell was transferred back to the protein sample and the pH adjusted to the next value by adding equal amounts of NaOH and 2x protein. The protein was mixed, and 70 μL of this solution was transferred to the microcell and the absorbance spectrum recorded again. This process was repeated from pH 2 to about pH 9. After measuring the absorbance at pH 9, the pH was adjusted to about 4.5 adding equal amounts of acid and 2x protein. The sample volume was then adjusted back to 2 mL by adding an appropriate volume of 2x protein, ddH_2O, and 6 M stock gdnHCl to achieve the next gdnHCl concentration. The titration was repeated as described above, except the pH was adjusted by adding NaOH, 3x-concentrated gdnHCl and 2x protein in a 1:2:3 ratio. The titrations were done at 0 M, 0.3, 0.6, and 0.9 M gdnHCl concentrations. For 0 M gdnHCl, the titrations were done from pH 2 to 9. For other [gdnHCl], the titrations were done from pH 4.5 to 9 due to precipitation problems in the presence of gdnHCl at lower pH values. The curves were fit to eq 3,

$$A_{695} = A_{695,alk} + \frac{[(A_{695,A} - A_{695,alk}) + (10^{-pK_{C1}}/(1 + 10^{n(pK_{a1}-pH)}))(A_{695,N} - A_{695,alk})]}{1 + \{10^{-pK_{C1}}/(1 + 10^{n(pK_{a1}-pH)})\}\{1 + [10^{-pK_{C2}}/(1 + 10^{(pK_{a2}-pH)})]\}} \quad (3)$$

where A_{695} is the observed absorbance at 695 nm during the alkaline transition, $A_{695,alk}$ is the absorbance at 695 nm of the alkaline state, $A_{695,A}$ is the absorbance at 695 nm of the acid state, $A_{695,N}$ is the absorbance at 695 nm of the Met 80-bound native state, K_C is the conformational equilibrium constant associated with the replacement of Met 80 with an alternative heme ligand, K_{C1} during the acid transition and K_{C2} during the alkaline transition, K_a is the acid dissociation constant linked to the conformational equilibrium, K_{a1} during the acid transition and K_{a2} during the alkaline transition, and n is the number of protons involved in the acid transition. The parameter, pK_{a1}, was arbitrarily set to 6 assuming H^+ dissociation from a histidine or a heme propionate. In fitting data, $A_{695,alk}$ was assumed to be equal to $A_{695,A}$ (lack of Met 80−heme binding), so the ($A_{695,A} - A_{695,alk}$) term in eq 3 disappears and the $A_{695,alk}$ and ($A_{695,N} - A_{695,alk}$) terms become $A_{695,A}$ and ($A_{695,N} - A_{695,A}$), respectively. When fitting data at other [gdnHCl], $A_{695,A}$ and ($A_{695,N} - A_{695,A}$) in eq 3 were set to the values obtained from fitting the 0 M gdnHCl data.

pH Jump Kinetics Experiments with the Stopped-Flow Technique. The experiments were done at 10 μM protein concentration in 100 and 500 mM NaCl. For the upward jumps, the initial pH of the protein was adjusted to pH 5.0 and then jumped from pH 5 to a final pH range of 6−10. The experiments were done using an Applied Photophysics π*-180 spectrometer with a stopped-flow unit operating in kinetics mode. The unit contained two equal volume syringes which pushed equal volumes of protein and the final pH buffer into the flow cell where the kinetics were measured. The protein stock solution was made with a final concentration of 20 μM in 100 or 500 mM NaCl. The buffers used to achieve the final pH were all 20 mM (MES, pH 6.0−6.6; $NaH_2PO_4 \cdot H_2O$, pH 6.8−7.6; Tris, pH 7.8−8.8; H_3BO_3, pH 9.0−10.0) made in 100 or 500 mM NaCl solution. For the downward jumps, the initial pH of the protein solution was adjusted to 8.0. The buffers for the downward jumps were made with acetic acid (pH 5.0 to 5.4) and MES (pH 5.6 to 6.4). For all buffers, pH was adjusted with HCl or NaOH as appropriate. The experiments were all done at 25 ± 0.1 °C (ThermoNESLAB RTE7 circulating water bath). The 20 μM protein and appropriate 20 mM buffer were mixed in 1:1 ratio to achieve the final pH, and after mixing, the protein was at 10 μM and buffer at 10 mM in 100 or 500 mM NaCl. The dead time of the instrument was measured by mixing 2,6-dichlorophenolindophenol with ascorbate at pH 2.0 (*33*) and was about 1 ms. The kinetic experiments were done by monitoring absorption at 406 nm, the wavelength of maximum change in absorbance for the conversion between native and the His 73-ligated alkaline state (*8*). For every pH, a minimum of 5 trials were done and a total of 5000 points were collected on a logarithmic time scale for each trial.

Analysis of the data was done using the curve fitting program SigmaPlot (v 7.0). Each trial of the upward pH jump data was fit using a double exponential rise to maximum equation (eq 4):

$$A_{406}(t) = A_{406}(0) + a_1(1 - \exp(-k_{obs,1}t)) + a_2(1 - \exp(-k_{obs,2}t)) \quad (4)$$

The downward pH jump data were fit using the equation for a double exponential decay (eq 5):

$$A_{406}(t) = A_{406}(\infty) + a_1 \exp(-k_{obs,1}t) + a_2 \exp(-k_{obs,2}t) \quad (5)$$

where $A_{406}(t)$ is the absorbance as a function of time at 406 nm, $A_{406}(\infty)$ is the absorbance at 406 nm at infinite time, $A_{406}(0)$ is the absorbance at 406 nm at time zero, a_1 and a_2 are amplitudes, and $k_{obs,1}$ and $k_{obs,2}$ are rate constants. k_{obs} and amplitude vs pH data were fit to the same mechanism used for the H73 variant previously (*21*):

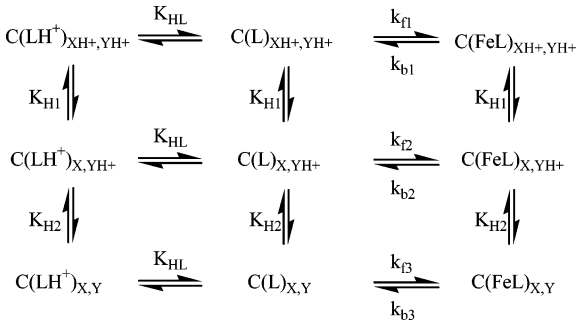

In this mechanism, C and C(FeL) represent the native and alkaline states, respectively, LH^+ and L represent the protonated and deprotonated forms of the ligand that replaces Met 80 in the alkaline state, and XH^+/X and YH^+/Y are the two ionizable groups that affect the rate of the conformational interconversion. K_{HL} is the ionization constant of the ligand replacing Met 80, and K_{H1} and K_{H2} are the ionization constants for the two additional trigger groups, X and Y, respectively. k_f and k_b are the forward and backward rate constants for the conformational change. The mechanism assumes that the ligand replacing Met 80 must ionize for the alkaline form to populate. Thus, the ligand is the thermodynamic trigger for formation of the alkaline state (*21*).

The rate constant data, k_{obs}, for upward and downward jumps were fit using eq 6, which is derived based on the above mechanism (*21*). In fitting data to this equation, the

$$k_{obs} = \left(\frac{K_{HL}}{K_{HL} + [H^+]}\right) \times \left(\frac{k_{f1}[H^+]^2 + k_{f2}K_{H1}[H^+] + k_{f3}K_{H1}K_{H2}}{K_{H1}K_{H2} + K_{H1}[H^+] + [H^+]^2}\right) + \left(\frac{k_{b1}[H^+]^2 + k_{b2}K_{H1}[H^+] + k_{b3}K_{H1}K_{H2}}{K_{H1}K_{H2} + K_{H1}[H^+] + [H^+]^2}\right) \quad (6)$$

equilibrium constant, pK_{C2}, at 0 M gdnHCl for the alkaline transition from eq 3 was used to constrain the ratios $k_{f1}/k_{b1} = k_{f2}/k_{b2} = k_{f3}/k_{b3} = K_{C2}$. The amplitude data were fit using eq 7, also derived from the above mechanism (*21*). In fitting data to this equation, only $[C_T]$ and K_{HL} were allowed to vary. The rate constants and acid dissociation constants were constrained to values obtained from the fit to eq 6.

$$\Delta A_{406} = [C_T] \times \left\{\frac{\left(\frac{K_{HL}}{K_{HL} + [H^+]}\right)}{\left(\frac{K_{HL}}{K_{HL} + [H^+]}\right) + \left(\frac{k_{b1}[H^+]^2 + k_{b2}K_{H1}[H^+] + k_{b3}K_{H1}K_{H2}}{k_{f1}[H^+]^2 + k_{f2}K_{H1}[H^+] + k_{f3}K_{H1}K_{H2}}\right)}\right\} \quad (7)$$

For the slow phase observed in the pH jump kinetics, the inflections in k_{obs} versus pH data caused by K_{HL} and K_{H1} were not well-resolved, so eq 6 did not converge well. Thus, k_{obs} versus pH data were fit to a simplification of the three trigger group equilibrium used to fit the fast phase from pH jump data which does not include K_{H1}:

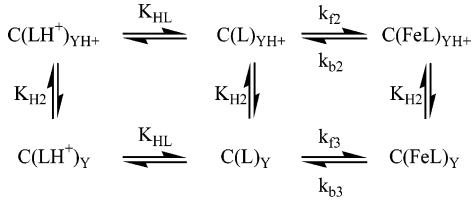

Equations 8 and 9 give the pH dependence for k_{obs} and amplitude, respectively (see ref *21* for derivations), where the parameters are as defined in eqs 6 and 7.

$$k_{obs} = \left(\frac{K_{HL}}{K_{HL} + [H^+]}\right)\left(\frac{k_{f2}[H^+] + k_{f3}K_{H2}}{K_{H2} + [H^+]}\right) + \left(\frac{k_{b2}[H^+] + k_{b3}K_{H2}}{K_{H2} + [H^+]}\right) \quad (8)$$

$$\text{amplitude} = [C_T]\left\{\frac{\left(\frac{K_{HL}}{K_{HL} + [H^+]}\right)}{\left(\frac{K_{HL}}{K_{HL} + [H^+]}\right) + \left(\frac{k_{b2}[H^+] + k_{b3}K_{H2}}{k_{f2}[H^+] + k_{f3}K_{H2}}\right)}\right\} \quad (9)$$

Analogous constraints are used in fitting data to eq 8 and 9 as for eq 6 and 7.

RESULTS

Global Unfolding by GdnHCl Denaturation. Global stability of the A79H73 protein was determined by using gdnHCl denaturation monitored by CD spectroscopy. The ellipticity measured at 222 nm plotted against the concentration of gdnHCl is shown in Figure 1. The fit of the data to eq 1 gives $\Delta G^o_u(H_2O) = 4.34 \pm 0.16$ kcal/mol, $m = 3.69 \pm 0.12$ kcal/(mol M) yielding a titration midpoint, $C_m = 1.17 \pm 0.04$, at pH 7.5 and 25 °C. These values are very similar to those observed for the H73 variant ($\Delta G^o_u(H_2O) = 4.32 \pm 0.11$ kcal/mol, $m = 3.59 \pm 0.01$ kcal/(mol M), $C_m = 1.15 \pm 0.01$ at pH 7.5 and 25 °C, see ref *6*). So, the Lys 79→Ala mutation has little effect on the global stability as monitored by gdnHCl denaturation and CD spectroscopy. The similarity of the *m*-values indicates that, as demonstrated for the H73 variant (*6*), the CD monitored unfolding occurs from a

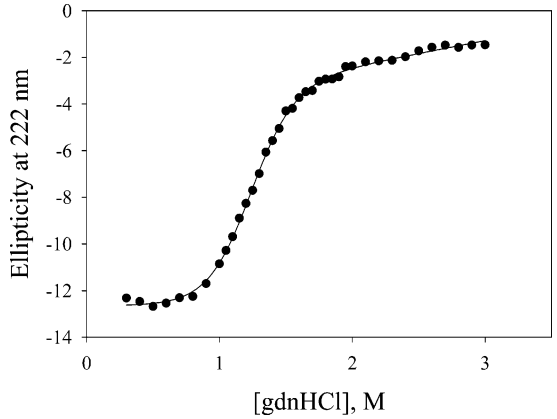

FIGURE 1: Plot of ellipticity at 222 nm versus gdnHCl concentration for A79H73 iso-1-cytochrome *c* monitored by CD spectroscopy. The experiment was done at pH 7.5 and 25 °C in 20 mM Tris, 40 mM NaCl buffer. The curve represents a nonlinear least-squares fit of the data to eq 1, Materials and Methods.

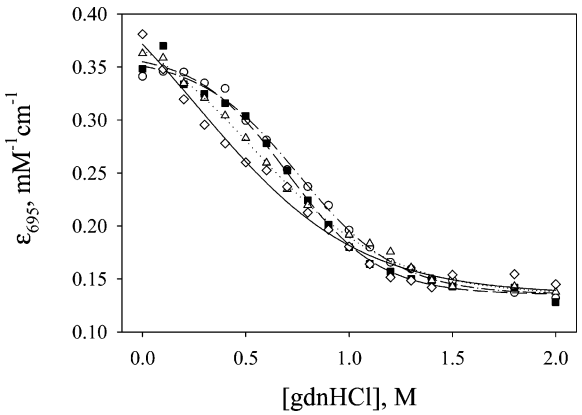

FIGURE 2: Plots of extinction coefficients at 695 nm (baseline corrected data) versus concentration of gdnHCl at different NaCl concentrations for the A79H73 variant, 40 mM (○), 100 mM (■), 200 mM (△) and 500 mM (◇). The curves are fits of the data (40 mM, dash−dotted; 100 mM, dashed; 200 mM, dotted; 500 mM, solid) to eq 2, Materials and Methods. All experiments were done at pH 7.5 and 25 °C in 20 mM Tris, 40 mM NaCl buffer.

partially unfolded form where Met 80 has been replaced by His 73 as the ligand at the 6th coordination site of the heme.

Partial Unfolding Monitored at 695 nm. Partial unfolding of the protein was studied at pH 7.5 using increasing concentrations of gdnHCl and monitoring the loss of Met 80−iron ligation at 695 nm. At pH 7.5, the equilibrium constant between the native state and the His 73 alkaline conformer is near 1 for the H73 variant. So, it was expected that addition of gdnHCl would cause an immediate drop in the absorbance at 695 nm for the A79H73 given the similarities in the CD-monitored gdnHCl unfolding of the A79H73 and H73 variants. In Figure 2, the extinction coefficient at 695 nm, ϵ_{695}, is plotted versus [gdnHCl] at various concentrations of NaCl. Surprisingly, the data show that, at 40 mM and 100 mM NaCl, the ϵ_{695} is constant at low gdnHCl concentrations. This constant ϵ_{695} region decreases as the salt concentration increases and essentially disappears at 500 mM salt concentration, where ϵ_{695} drops immediately as gdnHCl is added. The data suggest that there is salt stabilization of the native state relative to the His 73−heme alkaline conformer at low gdnHCl concentrations. Such stabilization was not observed for the H73 variant (*6*, *8*, *9*). At 500 mM NaCl, where ϵ_{695} versus [gdnHCl] begins to drop

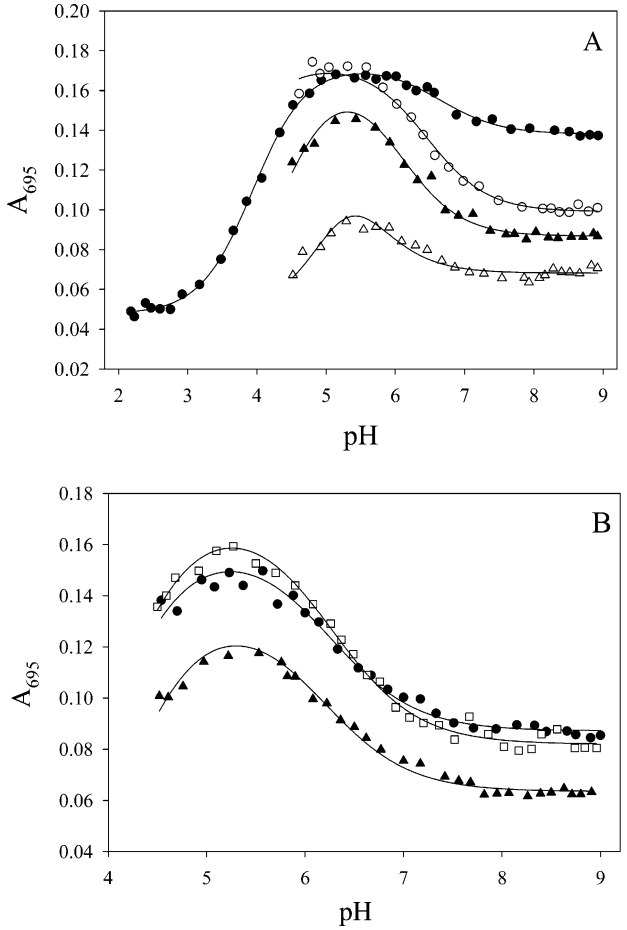

FIGURE 3: Plot of absorbance at 695 nm versus pH and [gdnHCl] for the A79H73 variant of iso-1-cytochrome *c* at 22 °C. (A) In the presence of 500 mM NaCl at 0 M (●), 0.3 M (○), 0.6 M (▲) and 0.9 M (△) gdnHCl. (B) In the presence of 100 mM NaCl at 0 M (●), 0.3 M (□) and 0.6 M (▲) gdnHCl. The solid curves represent nonlinear least-squares fits to eq 3. In all fits pK_{a1} for the group controlling the acid transition was taken to be 6. This choice is arbitrary and assumes the group is a heme propionate or a histidine.

immediately, the fit to eq 2 (Materials and Methods) yields $\Delta G^{o}_{u}(H_2O) = 0.4 \pm 0.3$ kcal/mol and $m = 1.5 \pm 0.3$ kcal/(mol M). These values are similar to those obtained previously for the H73 variant (*6*). However, since the native state baseline, $\epsilon_{695,N}$, is not well-defined, thermodynamic parameters obtained for partial unfolding are not completely reliable.

The data in Figure 2 also confirm that heme−Met 80 ligation is lost by 1.0 M gdnHCl, near the onset of CD-monitored unfolding (Figure 1). So, CD-monitored unfolding of A79H73 iso-1-cytochrome *c* is from a partially unfolded state.

Formation of the Alkaline Conformer as a Function of pH and GdnHCl Concentration. Another means of obtaining thermodynamic parameters for partial unfolding is to monitor the alkaline conformational transition as a function of [gdnHCl] (*8*, *31*). The absorbance at 695 nm was monitored as a function of pH at various gdnHCl concentrations. Data were obtained at both 100 mM and 500 mM NaCl to allow, respectively, comparison with previous data (*8*, *9*) and to provide thermodynamic data that is sensitive only to the denaturing properties of gdnHCl. The alkaline transition of the A79H73 variant at different concentrations of gdnHCl in 100 and 500 mM NaCl is shown in Figure 3. For the H73

Table 1: Thermodynamic Parameters for the Acid and Alkaline Conformational Transitions of the A79H73 Variant of Iso-1-cytochrome *c* at 22 ± 1 °C

	acid transition		alkaline transition	
[gdnHCl], M	pK_{C1}[a]	n[b]	pK_{a2}	pK_{C2}[c]
	100 mM NaCl			
0.0	−2.23 ± 0.09	1.09 ± 0.04	6.70 ± 0.03	−0.03 ± 0.08
0.3	−2.51 ± 0.09		6.89 ± 0.05	−0.17 ± 0.02
0.6	−1.62 ± 0.03		6.49 ± 0.04	−0.42 ± 0.02
	500 mM NaCl			
0.0	−2.34 ± 0.11	1.06 ± 0.12	6.5 ± 0.4	0.28 ± 0.19
0.3	−2.70 ± 0.16		6.84 ± 0.04	−0.17 ± 0.02
0.6	−1.71 ± 0.03		6.55 ± 0.04	−0.35 ± 0.02
0.9	−0.81 ± 0.03		6.16 ± 0.06	−0.71 ± 0.02

[a] pK_{C1} is the pK for the conversion of the acid state to the native state. pK_{a1} was arbitrarily set to 6 in fitting the data. So, pK_{C1} values are not absolute values. [b] n is the number of protons released in the acid to native transition. This value could only be measured at 0 M gdnHCl, so this value was used in fitting data obtained under all other conditions to eq 3. [c] pK_{C2} is the pK for the conversion of the native state to the alkaline state.

variant, a biphasic transition was observed with His 73 replacing Met 80 near neutral pH and Lys 79 replacing both His 73 and Met 80 at higher pH. The replacement of Lys 79 with Ala removes this second phase in the A79H73 variant (Figure 3). However, His 73−heme ligation is unable to drive the alkaline transition to completion at lower [gdnHCl], so it is not straightforward to determine $A_{695,alk}$, for complete loss of Met 80 at alkaline pH. On the other hand the acid transition results in a complete loss of absorbance at 695 nm in 0 M gdnHCl. So, in a single experiment, we monitor both the acid and alkaline conformational transitions of the A79H73 variant and make the assumption that the absorbance at 695 nm in the acid and alkaline states is the same ($A_{695,A} = A_{695,alk}$) since both correspond to complete loss of Met 80−heme ligation. Unfortunately, it was only possible to obtain data for both the acid and alkaline transitions at 0 M gdnHCl, due to precipitation problems in the presence of gdnHCl below about pH 4.5. So, the difference $A_{695,N} - A_{695,A}$ derived from 0 M gdnHCl data was used to fit all pH titration data to the following equilibrium (eq 3, Materials and Methods):

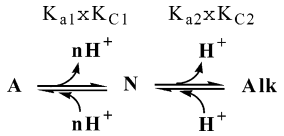

Parameters from data fits at both 100 and 500 mM NaCl are collected in Table 1. Consistent with His 73 replacing Met 80 as the heme ligand, a pK_a near 6.6 for the group triggering the alkaline transition is observed. As [gdnHCl] increases, the alkaline state becomes favored with respect to the native state (pK_{C2} becomes more negative) and the native state becomes less favored with respect to the acid state (pK_{C1} becomes less negative). In line with the effects of salt concentration seen in Figure 2, the stability of the alkaline state relative to the native state does not change strongly between 0 and 0.3 M in the presence of 100 mM NaCl (Figure 3B and Table 1). Similarly, there is no lag in the effect of [gdnHCl] on the stability of the alkaline state relative to the native state in the presence of 500 mM NaCl (Table 1, Figure 3A). Also, it is clear that in 0 M gdnHCl the His 73 alkaline state is not as well populated in 500 mM NaCl as in 100 mM NaCl (see Table 1, compare, Figures 3A and 3B). Thus, pH titration data confirm the observation in Figure 2 that salt stabilizes the native state relative to the alkaline state for the A79H73 variant.

The stability data for the alkaline state relative to the native state (pK_{C2} in Table 1) at 0.3 and 0.6 M gdnHCl show that both NaCl concentrations give comparable stabilities. So, the salt effect appears to be saturated at these combined concentrations of gdnHCl and NaCl.

A surprising aspect of the data in Table 1 is that the acid unfolding monitored at 695 nm is consistent with uptake of only one proton. In WT iso-1-cytochrome *c*, uptake of ∼2.6 protons occurs during acid unfolding (*7*). Closer inspection of the spectroscopic data shows that loss of Met 80 ligation (monitored at 695 nm) has been decoupled from formation of the high spin heme (monitored at 620 nm) typical of the acid denatured state (Figure S1, Supporting Information). In WT iso-1-cytochrome *c*, loss of Met 80 ligation and formation of the high spin heme at low pH occur simultaneously (*7*). For the A79H73 variant, the midpoint pH for loss of heme−Met 80 ligation is 4.0 and is an ∼1 proton process. Formation of the high spin heme at low pH has a midpoint pH of 3.0 and involves uptake of ∼1.6 protons. So, acid unfolding of the A79H73 variant goes through a stable intermediate.

Stopped-Flow Kinetic Studies of the Alkaline Transition of A79H73 Iso-1-cytochrome c. Kinetic studies were carried out to gain further insight into the alkaline transition caused by His 73−heme ligation using pH jump stopped flow methods. Data were acquired at both 100 and 500 mM NaCl. For the A79H73 variant we expect simpler kinetics than observed for the H73 variant (*21*), since Lys 79 is no longer present to complicate the interconversion between the native and His 73−heme alkaline state. Thus, there will be no interference from the formation of the Lys 79 alkaline conformer with the slow phase associated with formation of the His 73−heme alkaline conformer. This slow phase was attributed to cis/trans isomerization of Pro 76 (*21*). Since thermodynamic data on the A79H73 variant indicate that His 73 begins to displace Met 80 bound to heme at around pH 6.0, upward pH jumps were initiated at pH 5. Data were collected from a final pH of 6.0 to 10.0. Since the formation of the His 73−heme alkaline state is complete by pH 8.0, downward pH jumps were started at this pH. Figure 4 shows typical data for upward and downward pH jumps in the presence of 100 mM NaCl. Both upward and downward pH jumps show a fast phase occurring on an ∼100 ms time scale and a slow phase on an ∼10 s time scale.

Kinetic data for upward and downward pH jumps were obtained from pH 5 to 10, and rate constants and the amplitudes for fast and slow phases were extracted (Tables S1 to S16, Supporting Information). Figure 5 shows the pH dependence of the amplitude data for fast and slow phases for the upward pH jump data in 100 and 500 mM NaCl. Both phases at both NaCl concentrations increase in amplitude from pH 6 to 7.5, leveling off between pH 7.5 and 9, as seen for the growth of the alkaline conformer under equilibrium conditions (Figure 3). The pK of the ionizable group controlling the growth of this amplitude is near 6.5 in all cases (see caption to Figure 5), consistent with ionization

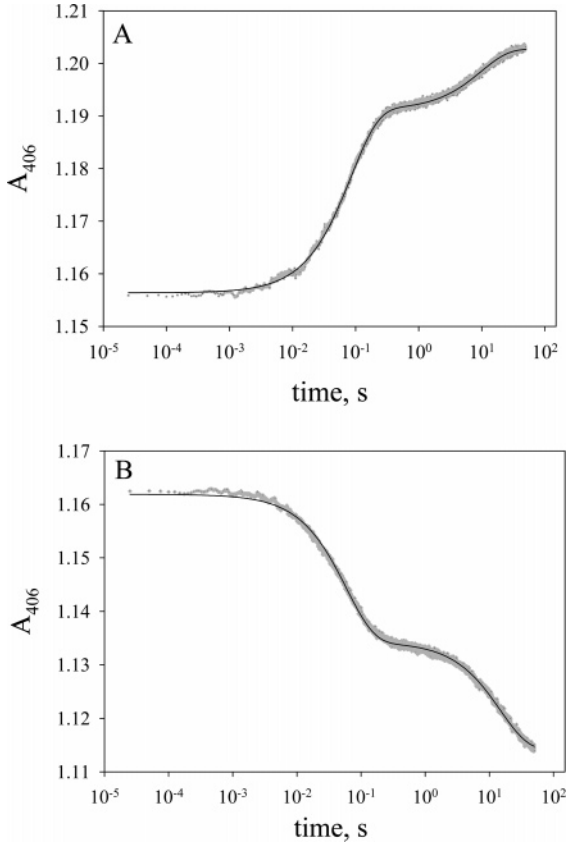

FIGURE 4: Plot of A_{406} versus time (on a logarithmic scale) for A79H73 iso-1-cytochrome *c* for (A) upward and (B) downward pH jumps in the presence of 100 mM NaCl at 25 °C. The upward pH jump was from pH 5 to 7 and the downward pH jump from pH 8 to 5.2. Data were collected at 406 nm with the protein concentration around 10 μM. The gray dots are the data at 406 nm, and the solid black curves are the fits of the data to double exponential rise to maximum (upward jump, eq 4 in Materials and Methods) or double exponential decay (downward jump, eq 5 in Materials and Methods) equations.

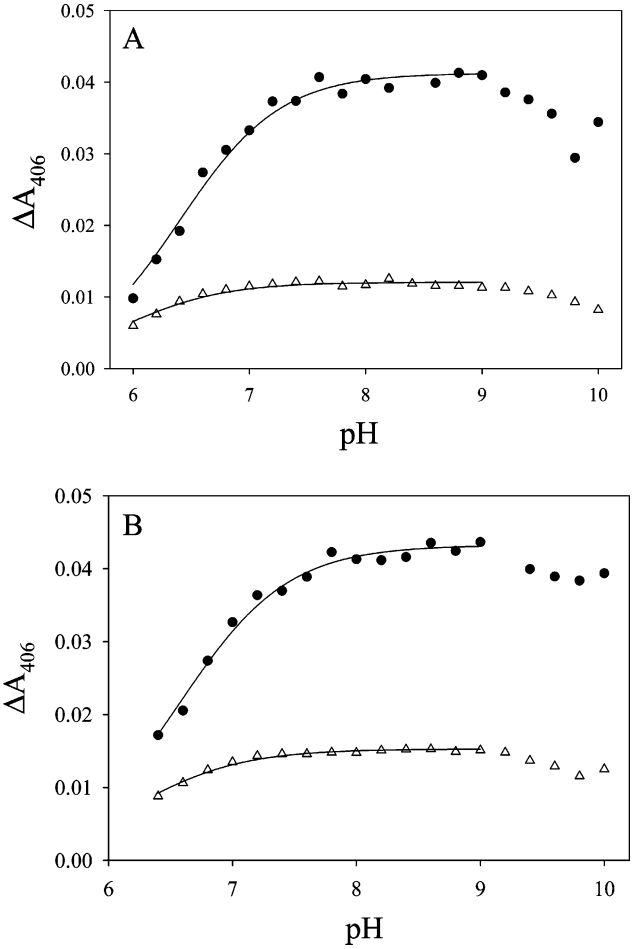

FIGURE 5: Plot of change in amplitude at 406 nm, ΔA_{406}, versus pH for the fast (●) and slow (△) phases of partial unfolding of the A79H73 variant for upward pH jump data in (A) 100 mM and (B) 500 mM NaCl. Data were collected at 406 nm in 100 mM NaCl at 25 °C with protein concentration around 10 μM. The solid curves in (A) are fits to the data from pH 6.0 to 9.0 using eq 7 (fast phase) or eq 9 (slow phase) in Materials and Methods. In fitting the data to eqs 7 and 9, rate constants from fits to eqs 6 and 8 in Figure 6 are used to parametrize eqs 7 and 9. Only pK_{HL} is obtained from the fit and is 6.75 ± 0.03 and 6.27 ± 0.05 for the fast and slow phases, respectively. The solid curves in part (B) are fits of the data from pH 6.4 to 9.0 to eqs 7 and 9 in Materials and Methods. In part (B), rate constants from fits of data in Figure 7 are used to parametrize eqs 7 and 9. pK_{HL} values obtained from the fit and are 6.76 ± 0.03 and 6.40 ± 0.02 for the fast and slow phases, respectively.

of a His 73 being the thermodynamic trigger for population of the alkaline state. The observation that the amplitudes of both the fast and slow phases grow synchronously with the population of the His 73−heme alkaline state in thermodynamic experiments (Figure 3) supports the assignment of both fast and slow phases to the formation of the His 73 alkaline conformer.

Above pH 9.0, the amplitudes for both the fast and slow phases decrease. Similar effects are observed in equilibrium titrations at pHs above 9 for both data monitored at 695 and 406 nm (data not shown). In equilibrium titration data, a shoulder starts to grow in rapidly at ~605 nm, above about pH 8.8, consistent with formation of a high spin heme (Figure S2, Supporting Information). These observations indicate that a weak field ligand begins to compete for binding to the heme above this pH. Spectra characteristic of a high spin heme have been observed during the alkaline conformational transition for other variants of iso-1-cytochrome *c* (*34*, *35*).

Figure 6 shows the pH dependence of the observed rate constant k_{obs}, for the fast and slow phases from both upward and downward pH jump data in 100 mM NaCl. As was observed for the H73 variant (*21*), k_{obs} for the fast phase decreases from pH 5 to 6, is relatively independent of pH from pH 6 to 8, and then increases again above pH 8. The slow phase does not change significantly between pH 5 and 6, increases between pH 6 and 8, and then increases again between pH 8 and 10. For the H73 variant (*21*), slow and intermediate phases were observable which could not be well-separated between pH 6 and 8 in upward pH jump data leading to uncertainties in the pH dependence of the slow and intermediate phases between pH 6.5 and 8. For A79H73 iso-1-cytochrome *c* only a single slow phase is observed providing for a well-defined pH dependence in this pH regime.

Figure 7 shows the pH dependence of the observed rate constant k_{obs}, for the fast and slow phases for both upward and downward pH jump data in 500 mM NaCl. The pH dependencies of k_{obs} for both phases are qualitatively similar to those observed in 100 mM NaCl. However, the drop in k_{obs} for the fast phase between pH 5 and 6 appears to be at somewhat higher pH and the plateau in k_{obs} between pH 6 and 8 is narrower (Figure 7A). Also, the k_{obs} values at 500

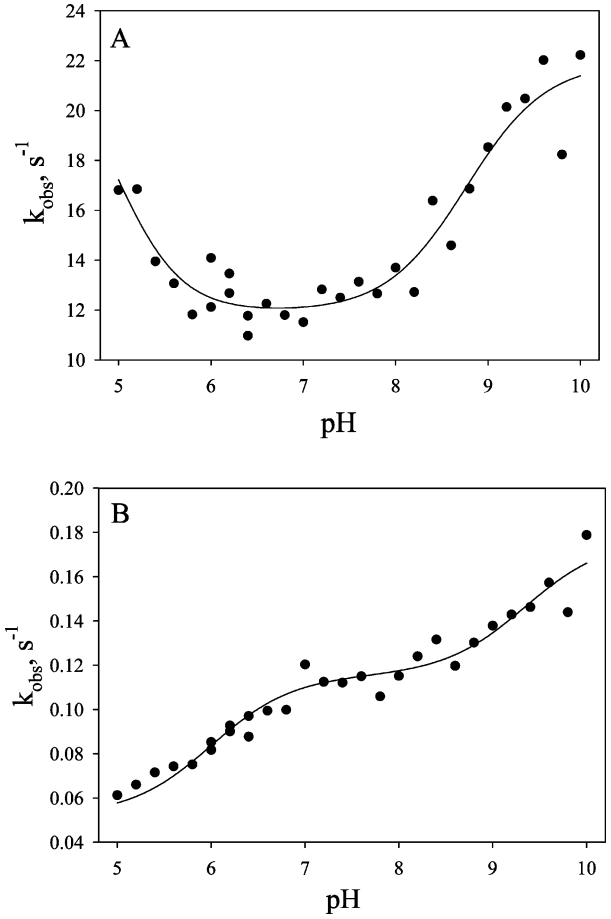

FIGURE 6: Plots of k_{obs} versus pH at 100 mM NaCl for the (A) fast and (B) slow phases of partial unfolding of the A79H73 variant to the His 73-ligated alkaline conformer for both upward and downward pH jump data. Data were collected at 25 °C with protein concentration around 10 μM at 406 nm. The solid curves are fits of the data to eqs 6 (fast phase) and 8 (slow phase) in Materials and Methods. The parameters from the fit are collected in Table 2.

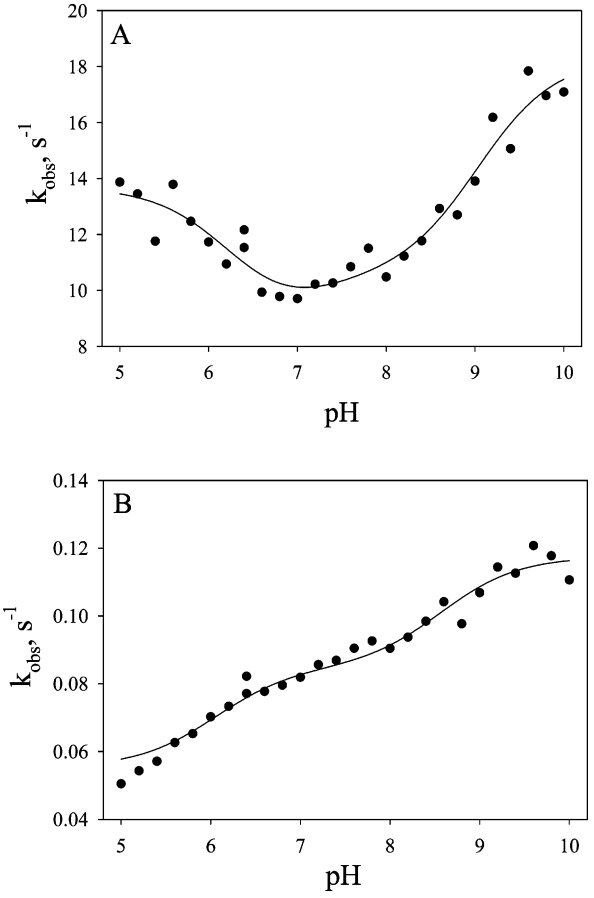

FIGURE 7: Plot of k_{obs} versus pH at 500 mM NaCl for the (A) fast and (B) slow phases of partial unfolding of the A79H73 variant to the His 73-ligated alkaline conformer for both upward and downward pH jump data. Data were collected at 406 nm at 25 °C with protein concentration around 10 μM. The solid curves are fits of the data to eqs 6 (fast phase) and 8 (slow phase) in Materials and Methods. The parameters from the fit are collected in Table 2.

mM NaCl are uniformly somewhat smaller in magnitude for both phases compared to data obtained in 100 mM NaCl.

DISCUSSION

Partial Unfolding of A79H73 Iso-1-cytochrome c. Experiments in 100 and 500 mM NaCl show that at pH 7.5 the native to His 73 alkaline state is poised at an equilibrium constant of about one (Figure 3 and Table 1). So, addition of gdnHCl to the A79H73 variant at pH 7.5 should lead to an immediate shift of the conformational equilibrium toward the partially unfolded (alkaline) form of the protein, as was observed for the H73 variant (*6*). Instead, the absorbance at 695 nm initially remains constant in the presence of 40 mM NaCl as the [gdnHCl] is increased (Figure 2). As salt concentration is increased, this plateau region slowly disappears consistent with a salt effect on this conformational transition. So, at lower gdnHCl concentrations, the ionic nature of gdnHCl predominates over its ability to denature proteins, apparently stabilizing the native state of the A79H73 variant. The stabilizing effect of gdnHCl at low concentrations, due to electrostatic interactions with the native state of proteins, has been observed for a number of proteins (*36*, *37*). Substitution of Lys 79 with the neutral amino acid alanine creates a site sensitive to such stabilization indicating that such effects can be predominately local.

The pH and gdnHCl dependence of the partial unfolding of the A79H73 variant to the alkaline conformer provides additional insight into the salt dependence of this process. Comparison of the data at 100 and 500 mM NaCl (Figure 3 and Table 1) shows that the stability of the native state relative to the His 73 alkaline conformer is less by ~0.4 kcal/mol ($\Delta\Delta G = \ln(10)RT\Delta pK_{C2}$) in 100 mM NaCl. After conversion of the pK values at 500 mM NaCl in Table 1 to free energies ($\Delta G = \ln(10)RT(pK)$), the partial unfolding data can be fit to a linear free energy relationship ($\Delta G_u(H_2O) = \Delta G_u - m$[gdnHCl]). The data for the alkaline transition yield an m-value of 1.4 ± 0.2 kcal/(mol M) and $\Delta G_u(H_2O) = 0.3 \pm 0.1$ kcal/mol. These values compare well to the m-value of 1.67 ± 0.08 kcal/(mol M) and $\Delta G_u(H_2O) = 0.38 \pm 0.01$ kcal/mol observed for formation of the His 73−heme alkaline conformer of the H73 variant (*8*). Thus, in 500 mM NaCl the properties of the alkaline transition of the A79H73 variant are similar to the properties of the transition from the native to the His 73−heme alkaline conformer of the H73 variant in 100 mM NaCl. So, increased salt concentration is able to reverse the destabilization of the native state relative to the alkaline state caused by conversion of lysine 79 to alanine.

Structural data for WT iso-1-cytochrome *c* (*38*) indicate that there are electrostatic interactions between the amino group of Lys 79 and the carboxyl group of the partially

buried heme propionate D (~4.8 Å from the Lys 79 amino group to nearest carboxylate oxygen of heme propionate D). When Lys 79 is replaced by Ala, these electrostatic interactions are lost and it leads to destabilization of the protein. Increased salt, NaCl or gdnHCl, appears to compensate for the loss of this electrostatic contact.

Mauk and co-workers have seen similar effects of salt on the alkaline transition of iso-1-cytochrome *c* (*5*). In their work, the most pronounced salt dependence at 0.1 M KCl and higher is for a Lys79→Ala variant (Lys 73 as heme ligand in the alkaline conformer). Between 0.1 and 0.5 M KCl the apparent p*K* of the alkaline transition increases by ~0.3 unit for this variant, consistent with the shift in pK_{C2} (Table 1) we see for A79H73 iso-1-cytochrome *c*. On the other hand the increase in the apparent p*K* of the alkaline transition for the WT protein is much less over this range of salt concentration (*5*), consistent with the lack of salt dependence observed for formation of the His 73-ligated alkaline conformer with the H73 variant. Thus, previous work on the alkaline transition also supports the importance of the Lys 79 to heme propionate D salt bridge for stabilizing the native state relative to the alkaline state for iso-1-cytochrome *c*.

Global Stability. The global stability monitored by CD spectroscopy indicates similar thermodynamic parameters, $\Delta G^{o}_{u}(H_2O)$ and *m*-value, for the H73 variant and the A79H73 variant. Comparison of Figures 1 and 2 shows that loss of Met 80 ligation is nearly complete when global unfolding monitored by CD spectroscopy starts. The *m*-values for both the H73 and the A79H73 variants are much smaller than the *m*-value of 5.1 ± 0.4 kcal/(mol M) observed for the WT protein (*39*). So, global unfolding proceeds from the His 73−heme alkaline conformer for both variants at pH 7.5. In accord with the observed separation of the partial and global unfolding steps, the *m*-values for partial unfolding to the alkaline conformer and "global" unfolding to the fully denatured state add up to the *m*-value for unfolding of the WT protein (1.4 + 3.6 = 5 kcal/(mol M)).

Perturbation of Acid Unfolding by the Lys 79→Ala Mutation. Previous studies on the acid unfolding of the H73 variant (*7*) show that the Lys 73→Ala mutation leads to partial separation of the loss of heme−Met 80 ligation and the formation of the high spin heme during acid unfolding. We attributed this loss in cooperativity during acid unfolding of H73 iso-1-cytochrome *c* to formation of a partially unfolded form with His 73−heme ligation based on thermodynamic arguments. For the A79H73 variant, the separation of these two transitions during acid unfolding is almost complete (Figure S2) indicating that addition of the Lys 79→Ala mutation leads to further loss of cooperativity. Heme propionate D is part of the buried hydrogen bond network of iso-1-cytochrome *c* (*38*), and it is possible that loss of the electrostatic contact to Lys 79 perturbs this network. Perturbations to the buried hydrogen bond network are known to strongly affect the stability of iso-1-cytochrome *c* (*40*, *41*). We have recently shown that mutations, which perturb this network, interact both cooperatively and anti-cooperatively with mutations at His 26 (*27*, *42*). These cooperative/anti-cooperative interactions correlate with changes in the length of a long-range hydrogen bond between the side chain of His 26 and the main chain carbonyl of Glu 44 caused by the mutations that affect the buried hydrogen bond network (*27*, *43*, *44*). Thus, a possible explanation of the observed loss in cooperativity of acid unfolding of the A79H73 variant is that the effects of the Lys 79→Ala mutation on the buried hydrogen bond network have weakened the His 26/Glu 44 hydrogen bond facilitating partial unfolding of the protein.

Amplitude of the Kinetics of the Alkaline Transition of A79H73 Iso-1-cytochrome c. As described in the Results section, the growth in the amplitude for both the fast and slow phases observed for interconversion between the native and the alkaline states is consistent with a histidine acting to trigger formation of the His 73-ligated alkaline conformer at both 100 and 500 mM NaCl. The kinetic models described in Materials and Methods are built around this requirement. When the amplitude data in Figure 5 are fit to this model, the p*K* values for this thermodynamic trigger (pK_{HL}) are near 6.5 (see caption to Figure 5). Thus, the pK_{HL} values obtained for the growth of the amplitude of the kinetics for the upward pH jumps (native to alkaline state kinetics) are consistent with ionization of His 73 acting as the thermodynamic trigger for formation of the alkaline state. This result is consistent with our results for the H73 variant (*21*).

pH Dependence of k_{obs} for the Fast Phase of the Alkaline Transition of A79H73 Iso-1-cytochrome c. As observed for the H73 variant, the pH dependence of k_{obs} for formation of the His 73-ligated alkaline conformer is more complicated than expected for a single ionizable trigger group. In the case of a single trigger group, k_{obs} is expected to increase from the rate constant of the back reaction, k_b, to the sum of the rate constants for the forward and back reactions, $k_f + k_b$, as the pH moves through the pK_a of the trigger group. As with H73 iso-1-cytochrome *c*, the fast phase is more complicated for the A79H73 variant at both 100 and 500 mM NaCl. A decrease in k_{obs} is seen at low pH at both NaCl concentrations, no change in the region where the amplitude of the alkaline conformer is increasing (compare Figure 5 with Figures 6 and 7), and then an increase in k_{obs} is observed again at high pH. Fits of the fast phase data for A79H73 iso-1-cytochrome *c* to the kinetic model used for the H73 variant yield k_f and k_b values and p*K*s for three ionizable groups (Table 2) as with the H73 variant (*21*).

First, we will consider the behavior of k_{obs} above about pH 6. The values obtained for pK_{HL} at 100 and 500 mM NaCl are near 6.5 as obtained for the rise in the amplitudes. The pK_{HL} values are also consistent with $pK_{HL} = 6.4 \pm 0.5$ obtained for H73 iso-1-cytochrome *c* (*21*). For pK_{H2}, the values obtained are similar to that obtained for the H73 variant (8.7 ± 0.2, see ref *21*). In comparing Figures 6A and 7A, it can be seen that k_{obs} ($k_f + k_b$) is somewhat higher above pH 6 in 100 versus 500 mM NaCl. The magnitudes of k_{b2} and k_{b3} do not change much at the two salt concentrations while k_{f2} and k_{f3} are twice as large at 100 mM NaCl as at 500 mM NaCl (Table 2). The increase in k_f at lower [NaCl] is consistent with the destabilization of the native state being due to loss of the electrostatic interaction between Lys 79 and heme propionate D in the A79H73 variant, as proposed above. At 500 mM NaCl, the k_{f2}, k_{b2}, k_{f3}, and k_{b3} values are very similar to the values obtained for H73 iso-1-cytochrome *c* at 100 mM NaCl ($k_{f2} = 3.5 \pm 0.2$, $k_{b2} = 7.0 \pm 0.4$, $k_{f3} = 6.6 \pm 0.2$, and $k_{b3} = 13.2 \pm 0.4$). Thus, high salt reverses the effects of loss of the electrostatic interaction between Lys 79 and heme propionate D.

Table 2: Kinetic Parameters for the Alkaline Transition of A79H73 Iso-1-cytochrome *c* at 25 °C[a]

	100 mM NaCl		500 mM NaCl	
	fast phase	slow phase	fast phase	slow phase
	Rate Constants, s^{-1}			
k_{f1}[b]	31 ± 26		7.2 ± 0.3	
k_{b1}	25 ± 21		13.7 ± 0.5	
k_{f2}	6.5 ± 0.3	0.064 ± 0.002	3.7 ± 0.4	0.029 ± 0.001
k_{b2}	5.4 ± 0.3	0.052 ± 0.001	7.0 ± 0.7	0.055 ± 0.002
k_{f3}	12.1 ± 0.5	0.097 ± 0.006	6.4 ± 0.3	0.041 ± 0.001
k_{b3}	9.9 ± 0.4	0.080 ± 0.005	12.0 ± 0.5	0.077 ± 0.002
	Ionization Constants			
pK_{H1}	5 ± 1		6.4 ± 0.2	
pK_{H2}	8.8 ± 0.2	9.3 ± 0.2	9.0 ± 0.2	8.6 ± 0.2
pK_{HL}	6 ± 1	6.0 ± 0.1	7.1 ± 0.5	6.0 ± 0.2

[a] In fitting k_{obs} versus pH data, the equilibrium constant for the native to His 73-ligated alkaline state, from fits of thermodynamic data in Figure 3, was used to constrain k_f/k_b. For 100 mM NaCl, $k_{f1}/k_{b1} = k_{f2}/k_{b2} = k_{f3}/k_{b3} = 1.22$. For 500 mM NaCl, $k_{f1}/k_{b1} = k_{f2}/k_{b2} = k_{f3}/k_{b3} = 0.53$. [b] The fit is only sensitive to k_{b1} in this pH regime (see ref *21*) and there is no direct evidence that k_{f1}/k_{b1} remains unchanged at low pH, so k_{f1} values should be interpreted with caution.

Below pH 6, the kinetics of the native/His 73-ligated alkaline state interconversion is dominated by the back reaction to the native state (k_b). In this pH regime, the A79H73 variant differs more strongly from the H73 variant. At 100 mM NaCl, pK_{H1} is lower and more poorly defined for the A79H73 variant than for the H73 variant (pK_{H1} = 5.6 ± 0.2, see ref *21*), whereas pK_{H1} is much higher for the A79H73 variant at 500 mM NaCl (see Table 2). k_{obs} is also uniformly higher for the H73 variant versus the A79H73 variant below pH 6. Thus, the enhancement of the back rate from the His 73-ligated alkaline state to the native state is significantly affected by the loss of the Lys 79/heme propionate D salt bridge.

The changes in pK_{H1} caused by the Lys 79→Ala mutation are likely related to the effects of this mutation on the acid unfolding transition discussed above. Both heme propionate D and His 26 have abnormal (and unknown) pK_a's in the native state of cytochrome *c* (*45*). Loss of the Lys 79/heme propionate D electrostatic contact and the effect that it has on the His 26/Glu 44 hydrogen bond is likely to perturb the pK_a's of these groups relative to WT iso-1-cytochrome *c*. Based on recent structural (*46*) and hydrogen exchange (*10*) data, both these contacts are likely to be broken or weakened in the alkaline state of cytochrome *c*. Since the normal pK_a's of heme propionates and histidines are ~5.2 (*45*) and ~6.5, respectively, the kinetics of formation of the native state from the alkaline state is likely to be modulated in the pH regime 5 to 6.5 by the effects of the Lys 79→Ala mutation on these groups.

pH Dependence of k_{obs} for the Slow Phase of the Alkaline Transition of A79H73 Iso-1-cytochrome c. In our work on H73 iso-1-cytochrome *c*, we assigned the slow phase associated with formation of the His 73-ligated alkaline state to cis/trans isomerization of Pro 76. This assignment is based on work on the folding of iso-2-cytochrome *c* which shows that conversion of Pro 76 to Gly eliminates a heme Soret-detected slow folding phase with a rate constant near 0.04 s^{-1} (*47*, *48*). In this work, we are able to observe the entire pH dependence of the slow phase. Figures 6B and 7B suggest that two ionizations affect k_{obs} as a function of pH. The fit of the data to a simpler kinetic scheme dependent on two ionizable groups (Table 2) yields pK_{HL} near 6 and pK_{H2} near 9 at both NaCl concentrations. These ionization constants are both reasonably consistent with the parameters obtained from fitting amplitude data (Figure 5) and the pH dependence of k_{obs} for the fast phase. The deviation of the data from the fit is significant for the low pH data (particularly at 500 mM NaCl, Figure 7B), most likely because pK_{HL} actually overlaps with pK_{H1} in this region such that the observed value of pK_{HL} from the fit has contributions from pK_{H1}. Thus, within error, the pK_{HL} and pK_{H2} ionizations are the same for both the fast and slow phases. The breakdown into k_f and k_b in Table 2 for a proline isomerization is probably not particularly meaningful; however, the pH dependence of the overall k_{obs} has some interesting trends. In both 100 and 500 mM NaCl, the low pH limit of k_{obs} is near 0.06 s^{-1}. However, at higher pH, k_{obs} is uniformly somewhat higher in 100 mM NaCl. Interestingly, the high pH limit for this proline isomerization slow phase is much faster for the H73 variant (~0.8 s^{-1}, see ref *21*), but the pK_{H2} is identical to that observed here (pK_{H2} = 8.8 ± 0.1, see ref *21*).

Implications for Proline Isomerization in Protein Folding. The pH dependence of k_{obs} for the slow phase that we attribute to isomerization of Pro 76 is in some sense surprising, since a hallmark of proline isomerization is that rates are independent of pH (*49*−*51*). k_{obs} should be dominated by cis to trans iomerization, k_{ct}, of the X-Pro 76 peptide bond for downward pH jumps which return the protein to the fully native state. For upward pH jumps, k_{obs} reflects the sum of k_{ct} and trans to cis, k_{tc}, isomerization. Since k_{ct} is typically 5 to 10 times larger than k_{tc} (*50*, *51*), the increase of k_{obs} with pH is much larger than might be expected. However, it is well-known that the conformation of a protein can affect the rate of isomerization of a given X-Pro peptide bond (*50*) causing both acceleration (*52*−*54*) and deceleration (*55*) of rates observed in unfolded proteins and peptides. In our system, pH changes the accessibility of different conformations.

For the slow phase observed here for the interconversion between the native and His 73 alkaline conformer of A79H73 iso-1-cytochrome *c*, the increase in k_{obs} appears to be coupled to the accessibility of the alkaline state in the pH range 6 to 8. This observation indicates that cis/trans isomerization at Pro 76 is more favorable in the more disordered alkaline conformer (*46*).

Above pH 8, the k_{obs} for the slow phase increases again (Figures 6B and 7B), yielding pK_{H2} near 9 at both 100 and 500 mM NaCl for A79H73 iso-1-cytochrome *c*. There are several features of pK_{H2} that are of interest. It is near the pH where the amplitudes of both the slow and fast phases begin to decrease. Evidence of a high spin heme begins to appear near pH 9 (shoulder at 605 nm). For H73 iso-1-cytochrome *c* (*21*), no loss of amplitude is observed for either the fast phase due to formation of the His 73 alkaline state or the associated slow phase attributed to Pro 76 isomerization. A possible explanation of these observations is that pK_{H2} is associated with a transient high spin intermediate with a conformation that enhances proline isomerization. For H73 iso-1-cytochrome *c*, this transient intermediate is less stable than the His 73 and Lys 79 alkaline forms up to pH 10. For A79H73 iso-1-cytochrome, however, this transient intermediate has significant equilibrium stability near pH 9 and above.

At high pH, k_{obs} for the slow phase is 0.12 to 0.18 s^{-1} (Figures 6B and 7B) about 4-fold slower than the maximal rate of ~0.8 s^{-1} observed for the H73 variant (*21*). For dihydrofolate reductase (*54*), folding studies coupled to mutagenesis indicate that hydrogen bond donation by nearby basic groups such as Arg, His, and Lys can act to promote proline isomerization. It is possible that Lys 79 acts to accelerate proline isomerization in the high spin intermediate proposed here such that replacement of Lys 79 in the A79H73 variant leads to a slowing of proline isomerization at high pH relative to the H73 variant.

Triggering the Alkaline Conformational Transition of Cytochrome c. The data on the kinetics of the alkaline transition of the A79H73 variant of iso-1-cytochrome *c* provide additional support for the three trigger group mechanism for the alkaline transition of cytochrome *c* seen in our previous work on the H73 variant (*21*). The substitution of Lys 79 with Ala in the A79H73 variant simplifies the kinetics allowing greater insight into the nature of this transition. In our earlier work (*21*), we concluded that ionization of His 73 (pK_{HL}) was required to permit population of the His 73 alkaline state and thus acted as a thermodynamic trigger for formation of this state. Our data on the A79H73 variant confirm this proposal.

In our work on the H73 variant (*21*), we did not attempt to assign the other triggering ionizations to specific groups. Recent studies on a set of iso-1-cytochrome *c* variants with substitutions for the heme ligand, Met 80 (*56*), show that formation of a low spin Fe(III)heme with His/OH^- ligation can occur with apparent pK_a's as low as 5.6 and as high as 12.9. These authors suggested that the pK_{H2} of ~8.7 observed in our work on the H73 variant might represent formation of an intermediate with His/OH^- heme ligation. Our current data, which show that a high spin intermediate begins to populate under equilibrium conditions above pH 9 in the A79H73 variant, appear to be inconsistent with this proposal. Our results are more in line with the data for a Trp 82 iso-1-cytochrome *c* variant where formation of a high spin intermediate is observed during the alkaline conformational transition (*35*). In the Trp 82 study, binding of deprotonated Tyr 67 to the heme is suggested as a likely candidate for the intermediate formed during the alkaline transition.

With regard to pK_{H1}, the Lys 79→Ala mutation significantly perturbs the effect of this ionization on the kinetics of the conversion between the native and alkaline states of the A79H73 variant versus the H73 variant. Below pH 6, where population of the alkaline state is minimal, k_{obs} primarily reflects k_{b1}. Since k_{b1} is slower for the A79H73 variant at both 100 and 500 mM NaCl than for the H73 variant, the effect of protonation (pK_{H1}) of the ionizable group is diminished by the Lys 79→Ala mutation. This decrease in k_{b1} presumably results from decreased stabilization of both the native and the transition states relative to the alkaline state. As discussed above, the Lys 79→Ala mutation is expected to impact the buried hydrogen bond network by breaking an electrostatic contact to heme propionate D, possibly weakening the His 26/Glu 44 hydrogen bond. Weakening this hydrogen bond would be expected to decrease k_{b1} by destabilizing both the native and the transition states relative to the alkaline state. Thus, we propose that pK_{H1} may reflect the formation of the His 26/Glu 44 hydrogen bond in the transition state between the native and alkaline state of cytochrome *c*.

SUMMARY

The thermodynamic and kinetic studies done on partial unfolding of the A79H73 variant show a monophasic alkaline transition, making the dynamics simpler than the H73 variant due to elimination of the Lys 79−heme alkaline conformer. The replacement of Lys 79 with Ala introduces a salt dependence to the partial unfolding mediated by His 73, indicating that Lys 79 electrostatically stabilizes the native state of cytochrome *c*. The pH jump kinetics of the alkaline conformational transition are also consistent with the proposal made for the H73 variant that two ionizable groups besides His 73 modulate the alkaline transition. Based on the properties of the A79H73 variant, we propose that the pK_{H1} ionization affects hydrogen bonding between the side chain of His 26 and the main chain of Glu 44 and that pK_{H2} reflects formation of a high spin Fe(III)−heme possibly with deprotonated Tyr 67 bound to the heme (*35*). Interestingly, the rate of a slow phase attributable to isomerization of Pro 76 appears to be promoted by population of the His 73 alkaline conformer and the proposed high spin Fe(III)−heme state. These results provide another example of the effect of protein conformation on rates of proline isomerization.

SUPPORTING INFORMATION AVAILABLE

Tables of rate constants and amplitudes for the A79H73 variant, comments on redistribution of amplitudes between the slow and fast phases in upward versus downward pH jump data, figure depicting acid transition of A79H73 at 695 versus 620 nm, and figure depicting pH dependence of absorbance spectra of A79H73. This material is available free of charge via the Internet at http://pubs.acs.org.

REFERENCES

1. Theorell, H., and Åkesson, A. (1941) Studies on cytochrome *c*, *J. Am. Chem. Soc. 63*, 1804−1820.
2. Greenwood, C., and Wilson, M. T. (1971) Studies on ferricytochrome *c*. 1. Effects of pH, ionic strength and protein denaturants on the spectra of ferricytochrome *c*, *Eur. J. Biochem. 22*, 5−10.
3. Wilson, M. T., and Greenwood, C. (1996) The alkaline transition in ferricytochrome *c*, in *Cytochrome c: A Multidisciplinary Approach* (Scott, R. A., Mauk, A. G., Eds) pp 611−634, University Science Books, Sausalito, CA.
4. Ferrer, J. C., Guillemette, T. G., Bogumil, R., Inglis, S. C., Smith, M. and Mauk, A. G. (1993) Identification of Lys79 as an iron ligand in one form of alkaline yeast iso-1-ferricytochrome *c*, *J. Am. Chem. Soc. 115*, 7507−7508.
5. Rosell, F. I., Ferrer, J. C., and Mauk, A. G. (1998) Proton-linked protein conformational switching: Definition of the alkaline conformational transition of yeast iso-1-ferricytochrome *c*, *J. Am. Chem. Soc. 120*, 11234−11245.
6. Godbole, S., Dong, A., Garbin, K., and Bowler, B. E. (1997) A lysine 73 → histidine variant of yeast iso-1-cytochrome *c*: Evidence for a native-like intermediate in the unfolding pathway and implications for *m* value effects, *Biochemistry 36*, 119−126.
7. Godbole, S., and Bowler, B. E. (1999) Effect of pH on formation of a nativelike intermediate on the unfolding pathway of a Lys 73 → His variant of yeast iso-1-cytochrome *c*, *Biochemistry 38*, 487−495.
8. Nelson, C. J., and Bowler, B. E. (2000) pH dependence of formation of a partially unfolded state of a Lys 73 → His variant

of iso-1-cytochrome *c*: Implications for the alkaline conformational transition of cytochrome *c*, *Biochemistry 39*, 13584−13594.
9. Nelson, C. J., LaConte, M. J., and Bowler, B. E. (2001) Direct detection of heat and cold denaturation for partial unfolding of a protein, *J. Am. Chem. Soc. 123*, 7453−7454.
10. Hoang, L., Maity, H., Krishna, M. M. G., Lin, Y., and Englander, S. W. (2003) Folding units govern the cytochrome *c* alkaline transition, *J. Mol. Biol. 331*, 37−43.
11. Bai, Y., Sosnick, T. R., Mayne, L., and Englander, S. W. (1995) Protein folding intermediates: Native-state hydrogen exchange, *Science 269*, 192−197.
12. Krishna, M. M. G., Lin, Y., Rumbley, J. N., and Englander, S. W. (2003) Cooperative omega loops in cytochrome *c*: Role in folding and function, *J. Mol. Biol. 331*, 29−36.
13. Davidson, V. L. (2002) Chemically gated electron transfer: A means of accelerating and regulating rates of biological electron transfer, *Biochemistry 34*, 14633−14636
14. Davidson, V. L. (2000) What controls rates of interprotein electron-transfer reactions?, *Acc. Chem. Res. 33*, 87−93.
15. Greenwood, C., and Palmer, G. (1965) Evidence for the existence of two functionally distinct forms of cytochrome *c* monomer at alkaline pH, *J. Biol. Chem. 240*, 3660−3663.
16. Wilson, M. T., and Greenwood, C. (1971) Studies on ferricytochrome *c*. 2. A correlation between reducibility and the possession of the 695 nm absorption band of ferricytochrome *c*, *Eur. J. Biochem. 22*, 11−18.
17. Hodges, H. L., Holwerda, R. A., and Gray. H. B. (1974) Kinetic studies of the reduction of ferricytochrome *c* by $Fe(EDTA)^{2-}$, *J. Am. Chem. Soc. 96*, 3132−3137.
18. Baddam, S., and Bowler, B. E. (2005) Conformationally gated electron transfer in iso-1-cytochrome *c*: Engineering the rate of a conformational switch, *J. Am. Chem. Soc. 127*, 9702−9703.
19. Döpner, S., Hildebrant, P., Rosell, F. I., and Mauk, A. G. (1998) Alkaline conformational transition of ferricytochrome *c* studied by resonance Raman spectroscopy, *J. Am. Chem. Soc. 120*, 11246−11255.
20. Döpner, S., Hildebrant, P., Rosell, F. I., Mauk, A. G., von Walter, M., Buse, G., and Soulimane, T. (1999) The structural and functional role of lysine residues in the binding domain of cytochrome *c* in the electron transfer to cytochrome *c* oxidase, *Eur. J. Biochem. 261*, 379−391.
21. Martinez, R. E., and Bowler, B. E. (2004) Proton-mediated dynamics of the alkaline conformational transition of yeast iso-1-cytochrome *c*, *J. Am. Chem. Soc. 126*, 6751−6758.
22. Deng, W. P. D., and Nickoloff, J. A. (1992) Site-directed mutagenesis of virtually any plasmid by eliminating a unique site, *Anal. Biochem. 200*, 81−88.
23. Smith, C. R., Mateljevic, N., and Bowler, B. E. (2002) Effects of topology and excluded volume on protein denatured state conformational properties, *Biochemistry 41*, 10173−10181.
24. Faye, G., Leung, D. W., Tatchell, K., Hall, B. D., and Smith, M. (1981) Deletion mapping of sequences essential for the *in vivo* transcription of the iso-1-cytochrome *c* gene, *Proc. Natl. Acad. Sci. U.S.A. 78*, 2258−2262.
25. Ito H., Fukada, Y., Murata, K., and Kimura, A. (1983) Transformation of intact yeast cells treated with alkali cations, *J. Bacteriol. 153*, 163−168.
26. Hammack, B. N., Smith, C. R., and Bowler, B. E. (2001) Denatured state thermodynamics: Residual structure, chain stiffness and scaling factors, *J. Mol. Biol. 311*, 1091−1104.
27. Redzic, J. S., and Bowler, B. E. (2005) Role of hydrogen bond networks and dynamics in positive and negative cooperative stabilization of a protein, *Biochemistry 44*, 2900−2908.
28. Bowler, B. E., May, K., Zaragoza, T., York, P., Dong, A., and Caughey, W. S. (1993) Destabilizing effects of replacing a surface lysine of cytochrome *c* with aromatic amino acids: Implications for the denatured state, *Biochemistry 32*, 183−190.
29. Bowler, B. E., Dong, A., and Caughey, W. S. (1994) Characterization of the guanidine hydrochloride-denatured state of iso-1-cytochrome *c* by infrared spectroscopy, *Biochemistry 33*, 2402−2408.
30. Pace, C. N. (1986) Determination and analysis of urea and guanidine hydrochloride denaturation curves, *Methods Enzymol. 26*, 266−280.
31. Kristinsson, R., and Bowler, B. E. (2005) Communication of stabilizing energy between substructures of a protein, *Biochemistry 44*, 2349−2359.
32. Schellman, J. A. (1978) Solvent denaturation, *Biopolymers 17*, 1305−1322.
33. Tonomura, B., Nakatani, H., Ohnishi, M., Yamaguchi-Ito, J., and Hiromi, K. (1987) Test reactions for a stopped-flow apparatus, *Anal. Biochem. 84*, 370−383.
34. Rosell, F. I., and Mauk, A. G. (2002) Spectroscopic properties of a mitochondrial cytochrome *c* with a single thioether bond to the heme prosthetic group, *Biochemistry 41*, 7811−7818.
35. Rosell, F. I., Harris, T. R., Hildebrand, D. P., Döpner, S., Hildebrandt, P., and Mauk, A. G. (2000) Characterization of an alkaline transition intermediate stabilized in the Phe82Trp variant of yeast iso-1-cytochrome *c*, *Biochemistry 39*, 9047−9054.
36. Makahatadze, G. I. (1999) Thermodynamics of protein interactions with urea and guanidinium hydrochloride, *J. Phys Chem. B 103*, 4781−4785.
37. Santoro, M. M., and Bolen, D. W. (1992) A test of the linear extrapolation of unfolding free energy changes over an extended denaturant concentration range, *Biochemistry 31*, 4901−4907.
38. Berghuis, A. M., and Brayer, G. D. (1992) Oxidation state-dependent conformational changes in cytochrome *c*, *J. Mol. Biol. 223*, 959−976.
39. Godbole, S., Hammack, B., and Bowler, B. E. (2000) Measuring denatured state energetics: Deviations from random coil behavior and implications for the folding of iso-1-cytochrome *c*, *J. Mol. Biol. 296*, 217−228.
40. Hickey, D. R., Berghuis, A. M., Lafond, G., Jaeger, J. A., Cardillo, T. S., McLendon, D., Das, G., Sherman, F., Brayer, G. D., and McLendon, G. (1991) Enhanced thermodynamic stabilities of yeast iso-1-cytochromes *c* with amino acid replacements at positions 52 and 102, *J. Biol. Chem. 266*, 11686−11694.
41. Linske-O'Connell, L. I., Sherman, F., and McLendon, G. (1995) Stabilizing amino acid replacements at position 52 in yeast iso-1-cytochromes *c*: *In vivo* and *in vitro* effects, *Biochemistry 34*, 7094−7102.
42. Wandschneider, E., Hammack, B. N., and Bowler, B. E. (2003) Evaluation of cooperative interactions between substructures of iso-1-cytochrome *c* using double mutant cycles, *Biochemistry 42*, 10659−10666.
43. Berghuis, A. M., Guillemette, J. G., McLendon, G., Sherman, F., Smith, M., and Brayer, G. D. (1994) The role of a conserved internal water molecule and its associated hydrogen bond network in cytochrome *c*, *J. Mol. Biol. 236*, 786−799.
44. Berghuis, A. M., Guillemette, J. G., Smith, M., and Brayer, G. D. (1994) Mutation of tyrosine-67 to phenylalanine in cytochrome *c* significantly alters the local heme environment, *J. Mol. Biol. 235*, 1326−1341.
45. Pielak, G. J., Auld, D. S., Betz, S. F., Hilgen-Willis, S. E., and Garcia, L. L. (1996) Nuclear magnetic resonance studies of class I cytochromes *c*, in *Cytochrome c: A Multidisciplinary Approach* (Scott, R. A., Mauk, A. G., Eds.) pp 203−284, University Science Books, Sausalito, CA.
46. Assfalg, M., Bertini, I., Dolfi, A., Turano, P., Mauk, A. G., Rosell, F. I., and Gray, H. B. (2003) Structural model for an alkaline form of ferricytochrome *c*, *J. Am. Chem. Soc. 125*, 2913−2922.
47. Wood, L. C., White, T. B., Ramdas, L., and Nall, B. T. (1988) Replacement of a conserved proline eliminates the absorbance-detected slow folding phase of iso-1-cytochrome *c*, *Biochemistry 27*, 8563−8568.
48. Pierce, M. M., and Nall, B. T. (1997) Fast folding of cytochrome *c*, *Protein Sci. 6*, 618−627.
49. Wedemeyer, W. J., Welker, E., Scheraga, H. A. (2002) Proline cis-trans isomerization and protein folding, *Biochemistry 41*, 14637−14644.
50. Balbach, J., and Schmid, F. X. (2002) Proline isomerization and its catalysis in protein folding, in *Mechanisms of Protein Folding* (Pain, R. H., Ed.) 2nd ed., pp 212−249, Oxford University Press, Inc., New York.
51. Reimer, U., Shere, G., Drewello, M., Kruber, S., Schutkowski, M., and Fisher, G. (1998) Side-chain effects on petidyl-prolyl cis/trans isomerisation, *J. Mol. Biol. 279*, 449−460.
52. Cook, K. H., Schmid, F. X., and Baldwin, R. L. (1979) Role of proline isomerization in the folding of ribonuclease A at low temperatures, *Proc. Natl. Acad. Sci. U.S.A. 76*, 6157−6161.
53. Schmid, F. X., and Blaschek, H. (1981) A native-like intermediate on the ribonuclease folding pathway. 2. Comparison of its properties to native ribonuclease A, *Eur. J. Biochem. 114*, 111−117.

54. Texter, F. L., Spencer, D. B., Rosenstein, R., and Matthews, C. R. (1992) Intramolecular catalysis of a proline isomerization reaction in the folding of dihydrofolate reductase, *Biochemistry 31*, 5687−5691.
55. Kiefhaber, T., Quaas, R., Hahn, U., and Schmid, F. X. (1990) Folding of ribonuclease T_1. 2. Kinetic models for the folding and unfolding reactions, *Biochemistry 29*, 3061−3070.
56. Silkstone, G. G., Cooper, C. E., Svistunenko, D., and Wilson, M. T. (2004) EPR and optical spectroscopic studies of Met80X mutants of yeast ferricytochrome *c*. Models for intermediates in the alkaline transition, *J. Am. Chem. Soc. 127*, 92−99.

BI0515873